

IMPACT EJECTA MODELING: MAIN PRINCIPLES AND A FEW EXAMPLES. N. Artemieva^{1,1}Institute for Dynamics of Geospheres, RAS, Moscow, ²Planetary Science Institute, Tucson, Arizona, artemeva@psi.edu, shuvalov@idg.chph.ras.ru.

Introduction: Most part of impact ejecta is deposited ballistically at some distance from a crater, defined by ejection velocity V and ejection angle α : $d=v^2\sin\alpha/g$. In case of giant impacts, planetary curvature should be taken into account [1]. Combined with ejecta scaling [2], these relations allow to define ejecta thickness as a function of distance. Ejecta from large craters are deposited at velocity high enough to mobilize substrate material and to thicken ejecta deposits [3]. Ballistic approximation is valid for airless bodies (if impact vaporization is not vast) or for proximal ejecta of large impact craters, where ejecta mass per unit area is substantially greater than the mass of involved vapor/atmosphere (M-ratio). Deposition of distal ejecta, in which ejecta mass is negligible compared to the atmosphere, may be also treated in a simplified manner, i.e. as 1) passive motion of ejected particles within an impact plume and 2) later, as sedimentation of particles in undisturbed atmosphere (equilibrium between gravity and drag). In all intermediate M-ratio values, impact ejecta move like a surge, i.e. dilute suspension current in which particles are carried in turbulent flows under the influence of gravity. Surges are well-known for near-surface explosive tests, described in detail for volcanic explosions (Plinian column collapse, phreato-magmatic eruption, lateral blast), and found in ejecta from the Chicxulub [4] and the Ries [5]. Important aspects of surge transport include its ability to deposit ejecta over a larger area than that typical of continuous ballistic ejecta and to create multiple ejecta layers.

Numerical models. Surges should be modeled in the frame of two-phase hydrodynamics, i.e. interaction between solid/molten particles and atmospheric gas/impact vapor should be taken into account. There are two techniques of solving equations for dust particle motion in a gas flow. The first one describes solid/molten particles as a liquid with specific properties, i.e. finite-difference equations are the same as in standard hydrodynamics [6-7]. This approach is quite simple, but has some limitations such as low resolution, strong numerical diffusion, and impossibility to describe particles of different size within one computational cell. The latter disadvantage is overcome in [8], but the price is the much greater number of equations to be solved and, hence, more arrays to be stored.

Another approach is based on solving equations of motion for representative particles [9]. Each of these

markers describes the motion of a large number of real particles with similar sizes, velocities, and trajectories. Equation of motion (gravity, viscosity, and drag) is solved for every marker and then exchange of momentum, heat and energy with surrounding vapor-air mixture is taken into account. This approach is used in the SOVA code [10] and allows to vary particle sizes within a broad range (from a few m to a few microns). Implicit procedure of velocity update allows a larger time step. The substantial advantage of the model is its three-dimensional geometry, allowing modeling of asymmetric deposits of oblique impact ejecta. Turbulent diffusion is taken into account in a simplified manner [6].

Fragments size-frequency distribution (SFD) may be of crucial importance: while large fragments move ballistically, the smallest ones are passively involved in gas motion. Ejected material is usually transformed into particles under tension. The initial particle velocity is given by the hydrodynamic velocity, but the object's initial position within the cell is randomly defined. The SFD of solid fragments in high velocity impacts has been studied experimentally [2,11], numerically [12,13], and has been derived from the lunar and terrestrial crater observations [14,15]. Standard cumulative SFD ($N\sim D^{-b}$) is a consequence of the entire process, i.e., it represents the sum of individual ejection events taking place through time and space. Various approaches may be used to implement fragment size in a dynamic model: in Grady-Kipp model the average fragment size is defined by strain rate [12]; alternatively, average ejection velocity [16] or maximum shock compression [17] may be used. All methods may be verified through comparison with known data.

Volcanic direct blast. Numerical modeling of pyroclastic flows, checked against recent observations and young deposits, may be then a useful instrument for reconstruction of terrestrial craters' ejecta, which are mostly eroded or buried; and for impact ejecta study on other planets (first of all – on Mars), where remote sensing data are still the only source of our knowledge. In volcanology typical velocities are usually below 300 m/s, temperatures may be as low as 300 K (wet surge) and not higher than 1000 K (dry surge), solid/gas mass ratio ranges between 5-50, particle size rarely exceeds several cm, while the mass fraction of fine micron-sized particles is usually poorly defined.

Fig. 1 shows modeled direct blast at Bezymianny volcano (Kamchatka, Russia) in 1956.

Crater ejecta. Impact ejecta parameters vary in a substantially wider range: distal ejecta velocities reach several km/s, km-sized fragments are typical for large craters, gas content may be high enough for cratering in volatile rich (or water-covered) target or in the presence of a dense atmosphere.

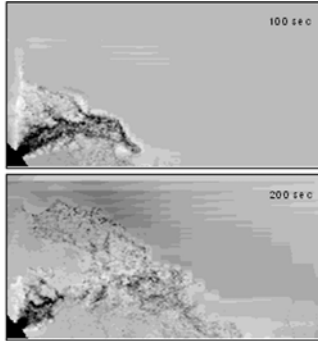


Fig.1 Directed blast at Bezymianny volcano (1956). Ejected material in atmosphere for tephra/gas ratio at the vent of 20. Modeled deposited area extends to 20-30 km from the vent and has a width of 10-15 km in a reasonable agreement with geological observations.

Moldavites from the Ries crater. The Ries impact site is characterized by a thick sedimentary layer, from which a large amount of vapor (e.g., CO₂) is shock-released. This vapor contributes to the ejected particles acceleration, or at least, to the sustainment of their motion. The initial ejection velocities of material are rather high, up to 10 km/s, which are close to the velocity of the expanding gas. As a result, the particles are not subject to high dynamic pressures (Fig. 2) that otherwise would disrupt them into fine mist immediately after ejection. The temperature of the entraining gas is rather high, so the particles do not cool quickly during the flight, allowing enough time to have them aerodynamically shaped (typical for tektites), and to lose volatiles [18,19]. Tektites are distributed up to 400-500 km away from the impact, in a fan of ~75° symmetrically distributed with respect to the down-range direction.

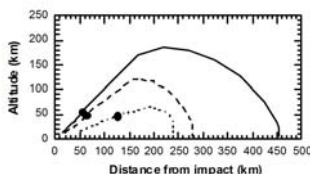


Fig.2 Trajectory of tektites in Earth's atmosphere. Molten cm-sized particles move within an impact plume without drag and are deposited by fallout hundreds km away from parent crater.

Chicxulub distal ejecta. We model the Chicxulub crater formation and use ballistic continuation to define ejecta thickness and composition as a function of a distance from the crater. The total amount and estimated thickness of ejecta is comparable with observations, with a few cm at intermediate distances of 1800-

2500 km (e.g. in North America), and a few mm thick worldwide (at distances > 4000 km). However, ejecta thickness decreases with distance in contradiction with observations (2-3 mm world-wide). We also do not have any basement material in distal ejecta, as ejection velocity from a depth of 3 km is lower than 3.5 km/s. To find better correlation with observations, we suggest additional re-distribution of ejecta by floating of impact debris above the atmosphere [20,21].

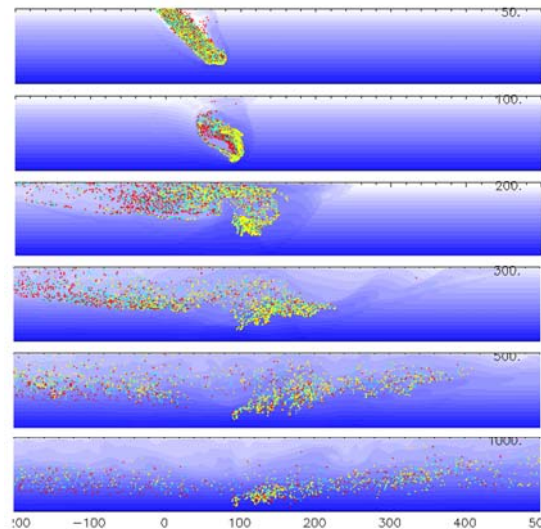


Fig.3 Chicxulub ejecta. Shock waves in atmosphere and dispersion of re-entry ejecta. Atmosphere thickness (Y-axis) is 100 km, numbers along the X-axis show distance from the re-entry point in km. Y-scale shows 100 km of the Earth's atmosphere. Numbers in the upper right corner of each snapshots – time in seconds.

References: [1] Dobrovolskis A. (1981) *Icarus* 47, 203–219. [2] Cintala M.J., et al. (1999) *M&PS* 34, 605–623. [3] Oberbeck V.R. (1975) *Rev. Geophys. Space Phys.* 13, 337-362. [4] Dressler et al. (2004) *M&PS* 39, 857-878. [5] Hörz F. et al. (1983) *Rev. Geophys. Space Phys.* 21, 1667-1725. [6] Valentine G.A. and Wohletz K.H. (1989) *JGR* 94, 1867-1887, [7] Dobran F. and Neri A. (1993) *JGR* 98, 4231-4259. [8] Neri A. et al. (2003) *JGR* 108, doi:10.1029/2001JB000508. [9] Boothroyd R.G. (1971) *Flowing gas-solids suspension*, Chapman and Hall Ltd, London. [10] Shuvalov V.V. (1999) *Shock waves* 9, 381-390. [11] Nakamura A. and Fujiwara A. (1991) *Icarus* 92, 132–146. [12] Grady D.E. and Kipp M.E. (1980) *Int. J. Rock Mech. Min. Sci. Geomech. Abstr.* 17, 147–157. [13] Melosh H.J. et al. (1992) *JGR* 97, 14735–14759. [14] Gault, D.E. et al. (1963) *NASA TND-1767*. [15] Vickery A.M. (1986) *Icarus* 67, 224–236. [16] Melosh H.J. (1984) *Icarus* 59, 234–260. [17] Shuvalov V.V. (2002) *LPSC-33*, abstr.#1259. [18] Stöffler et al. (2002) *M&PS* 37, 1893-1908. [19] Melosh H.J. and Artemieva N.A. (2004) *LPSC-35*, abstr. #1723. [20] Colgate S.A. and Petschek A.G. (1985) *LA-UR-84-3911*. [21] Artemieva N. and Morgan J. (2008) *LPSC-39*, abstr. # 1581.